

NEUROExos: a variable impedance powered elbow exoskeleton

Tommaso Lenzi, *Student Member IEEE*, Nicola Vitiello, Stefano Marco Maria De Rossi, *Student Member IEEE*, Stefano Roccella, Fabrizio Vecchi, *Member IEEE*, Maria Chiara Carrozza, *Member IEEE*

Abstract—This paper introduces NEUROExos, an elbow powered exoskeleton for rehabilitation. The NEUROExos is provided with three novel characteristics which address the major problems arising in rehabilitation robotics. A double-shell link structure allows for a comfortable human-robot interaction, while a 4-DOF passive mechanism gives a perfect kinematic compatibility with the user. Moreover, NEUROExos is powered by a variable impedance antagonistic actuator, which provides the exoskeleton with a software-controllable passive compliance. We present the main characteristics of the exoskeleton, with a focus on the actuation and control of the platform. Additionally, results on a healthy subject show the relevance of this design during a prototypical rehabilitation task.

I. INTRODUCTION

THE cerebrovascular accident, or stroke, is one of the five main chronic diseases identified by the World Health Organization (WHO) in their 2008 report [1]. Each year, approximately 500,000 people experience a stroke in US and about 1.1 million in Europe [2], [3]. This high incidence, combined with an aging population, significantly strains national healthcare services and related costs [4].

A potential consequence of the stroke is the impairment of the motor function of the upper limb, and then the difficulty to perform activities of daily living [5]. A therapeutic treatment consisting of highly repetitive movements of the impaired limb is one of the most effective approaches to partly restore the motion abilities [6]. Unfortunately, this strategy is labor-intensive, requires one-to-one therapist-patient interaction and gives results after several weeks of treatment. Therefore, the provision of highly intensive treatment for all the patients becomes onerous.

Given that, many research groups investigated on the development of new robotic platforms to support the therapist in providing high-intensity and repetitive therapy, and to provide an objective, reliable means of monitoring the patient progress. Relying on this idea, in the last decades,

Manuscript received Sept 15th 2010. This work was partly supported by the EU within the NEUROBOTICS Integrated Project (The fusion of NEUROscience and roBOTICS, IST-FET Project #2003-001917) and within the EVRYON Collaborative Project STREP (Evolving Morphologies for Human-Robot Symbiotic Interaction, Project FP7-ICT-2007-3-231451).

T. Lenzi, N. Vitiello, S.M.M. De Rossi, S. Roccella, F. Vecchi, M.C. Carrozza are with ARTS Lab, Scuola Superiore Sant'Anna, viale Rinaldo Piaggio, 34, 56015, Pontedera (PI), Italy. (Tommaso Lenzi is the corresponding author; phone: +39 050 883472; fax: +39 050 883497; emails: t.lenzi@sssup.it).

E-mails: n.vitiello@sssup.it, s.derossi@sssup.it, s.roccella@sssup.it, f.vecchi@sssup.it, carrozza@sssup.it.

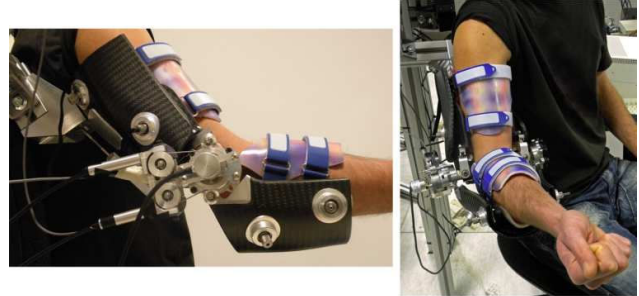


Fig. 1 Overview of NEUROExos platform.

robot-aided neurorehabilitation was widely investigated and proved to be good as or even better than conventional therapy [7].

State-of-the-art devices for upper limb robot-assisted therapy can be classified in: end-point manipulators [8], cable suspensions [9] [10], and exoskeletons [11] [12]. Among these, the latter was proposed as a solution to the problem of control and measurement of angle and torque on each joint of the impaired limb [13], which is a basic requirement for a successful rehabilitation therapy.

An exoskeleton is a wearable mechatronic system matching the shape and the function of the human limb to be assisted [12]. Wearability is one of the most critical design requirements for this kind of robot. The kinematic structure of a wearable exoskeleton should take into account the natural variability of the users' anthropometry, the range of motion of the limbs, and also the intra-subject variability of the joint center of rotations during movements [13]. Additionally, the whole mechanism should have overall low inertia, weight and encumbrance. Additional requirements are related to the interaction surface between the user and the robot, which should be large and have a good match with the shape of the patient's limb. This way the pressure on the users' skin is kept low, reducing the risk of uncomfortable patient-robot interaction [14]. Finally, the actuation system should guarantee sufficient force/torque performances to execute the rehabilitation task while allowing for a safe patient-robot interaction even in case of spasmodic motion [15].

In this paper we present NEUROExos (NEUROBOTICS Elbow Exoskeleton), an elbow exoskeleton for neuro-rehabilitation purposes. This wearable robot, shown in Fig. 1, possesses many innovative features which fulfill the aforementioned design requirements. These features, which will be described in Section II, are:

1. a double-shell link structure, which improves the robot wearability and comfort by reducing the pressure on

the user's skin;

2. a passive self-aligning mechanism, which allows the actuated joint axis to be always aligned with the instantaneous human joint rotation axis;
3. a bio-inspired compliant actuation system able to regulate independently the actuated joint position and stiffness, in an open-loop fashion.

Section III will introduce the bio-inspired control algorithm for the passive compliance and position regulation, which experimental characterization will be reported in Section IV. In Section V, a prototypical rehabilitation task will be tested on a healthy volunteer in order to show a practical application of the NEUROExos features. Finally, Section VI will draw the conclusions.

II. THE NEUROEXOS PLATFORM

A. The double-shell link structure

NEUROExos links are designed to fit the shape of the user's limb segments and distribute the interaction force between the user and the robot over a wide area. This allows to reduce the pressure on the user's skin and ensure a comfortable and safe interaction. High localized pressure values can indeed be felt as uncomfortable or even painful by the user, as shown in [16]. The NEUROExos links are depicted in Fig. 2. Each link is composed of a two-layered shell structure [17][18]. The inner shells are tailor-made on each subject and are in contact with the arm segments. The external shells are the same for different subjects, and constitute a rigid frame.

Each inner shell is made of two half-shells, to be coupled with the dorsal and ventral sides of the limb segment. In this way, the user can easily wear the exoskeleton by laying down his/her arm on the dorsal half-shells, and then fastening the ventral half-shells to the arm with two velcro

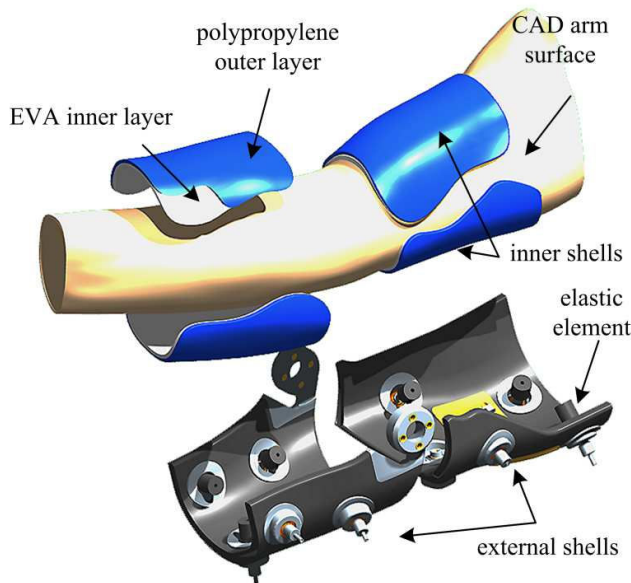


Fig. 2 Exploded view of the double-shell structured links.

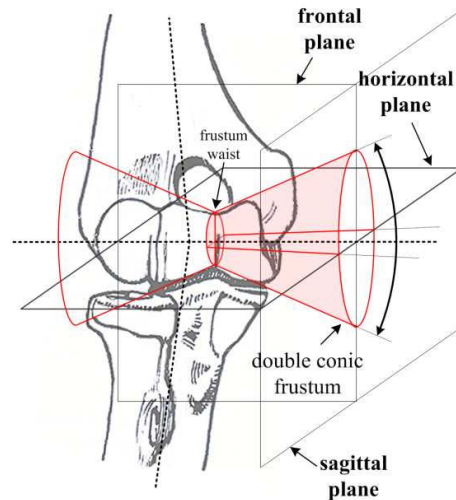


Fig. 3 Anatomy of the elbow articulation with the double shell frustum in evidence (adapted from I.A. Kapandji).

belts, as depicted in Fig. 1. The inner shells have a two layered structure: a 3 mm-thick internal layer of ethylene vinyl acetate, EVA, (555XEB/3, M.T.O., Italy), for moisture draining and skin transpiration, and a 3 mm-thick outer layer of polypropilene (558/3 M.T.O., Italy).

The external shells have a double-wall carbon fiber structure of two 1.5 mm-thick layers spaced by 7 millimeters. This solution guarantees an overall low encumbrance, weight and inertia as well as a high torsional and flexional stiffness required to provide the interaction torque. The external shells are linked with the inner shells through four elastic connecting elements, which are screwed, on one side, to the polypropylene layer of the inner shell and, on the other side, to a spherical joint that is housed by an aluminum frame inserted on the carbon fiber structure of the outer shell (see Fig.2). Thanks to a high longitudinal compression stiffness (100 N/mm), the elastic elements can transmit the interaction force between the inner and the outer shells while allowing, at the same time, small relative motions thanks to a lower shear stiffness (15 N/mm).

B. The passive self-aligning mechanism

Orthopedic studies demonstrate that human elbow is a 'loose hinge joint' over its motion range. Because of its laxity, the elbow rotation axis traces the surface of a double quasi-conic frustum with an elliptical cross-section [19] (see Fig. 3). This conic frustum varies in shape among subjects, and also within an individual subject depending on the flexion mode (active/passive), the forearm position (pronosupination angle) and the presence of varus or valgus moments applied on the forearm during the elbow motion.

In order to avoid undesired interaction forces and ensure a good kinematic compatibility over all possible elbow movements, we introduce redundant degrees of freedom on the exoskeleton. Instead of decoupling the joint rotations from the joint translations, as in [13], we designed a 4-DoF passive mechanism which provides the actuated-joint

rotation axis with two rotational and two translational degrees of freedom. The range of motion of this passive mechanism covers the variability of the human frustum and therefore ensures a perfect kinematic compatibility between the robot and the user during motion. An accurate description of this mechanism, along with its experimental validation on end-users, is out of the scope of this paper and will be presented in detail on [20]. For a demo of the NEUROExos passive mechanism see <http://db.tt/MYkE0HI>.

C. The antagonistic actuation system

Compliant actuation is claimed to be one of the main requirement for a rehabilitation device [21]. Differently from closed-loop controlled rigid actuator, it guarantees low output impedance, even in case of high frequency disturbances [22]. This is particularly important when a spasmodic event happens. In this case, the patient would interact with a compliant device, avoiding any risk of suddenly high and painful interaction forces. Compliant actuation systems such as series elastic actuators [23] have been widely applied in this field [24]. While this solution is inherently not rigid, variations in the output impedance can be achieved only by means of closed-loop interaction control strategies [25]. To overcome this limitation, variable impedance actuators have been proposed [26]. These actuators simplify the control system and provide the joint with software-controllable hardware compliance. The resulting adjustable compliant behaviour is an inherent hardware property of the actuation system and does not require any additional control loop.

NEUROExos is provided with an adaptive, passive-compliant actuator [27], implemented by means of an antagonistic non-linear elastic actuation system. This configuration takes inspiration from human musculoskeletal system, which powers the limbs through antagonistic muscle pairs. The musculoskeletal system generates a convergent force field around an equilibrium position of the limb by relying on the elastic features of antagonistic muscles. The selective activation of one of the two muscles displaces the convergent field towards a new equilibrium position and, consequently, changes the position of the limb. The simultaneous co-activation of both muscles (i.e. muscles co-contraction) increases the slope of the convergent field (i.e. the joint stiffness), leaving the limb position unchanged [28][29]. In a similar way, the actuation system of NEUROExos can apply a convergent torque field around a certain angular position (i.e. the equilibrium point) by regulating the rest lengths of two opposite elastic actuation lines. The slope of this convergent torque field (i.e. the joint stiffness) can be regulated independently to the equilibrium position, thanks to the non-linearity of the compliant elements [26].

The layout of the actuation system of NEUROExos consists of a pair of remote and independent antagonistic units as depicted in Fig. 4-a. Each unit consists of a series of: a non-linear elastic element having a quadratic force (F) vs. cable elongation (Δl) characteristics (i.e. $F(\Delta l) = b_1 \Delta l^2 + b_2 \Delta l^2$), a linear hydraulic actuator with a

stroke of 50 millimeters (Parker-Hannifin Corp., OH, USA), a stroke amplifier (transforming an hydraulic piston displacement Δx in an elongation of the transmission $\Delta l = a_s \Delta x$, with $a_s = 4$), and a steel-wire rope with a diameter of 1.4 millimeters (Carl Stahl, Süssen, Germany) which transmits the force to the NEUROExos driving block through Bowden cable. Each hydraulic cylinder is controlled by a three-land-four-way proportional electronic valve, commanded by a ± 10 V DC signal, which sets the spool valve position, and consequently the piston velocity, as explained in [30]. The hydraulic circuit is powered by a three-phase 1.1 kW AC motor (Parker-Hannifin Corp., OH, USA).

The non-linear elastic element is based on a linear tension spring coupled with a cam mechanism (see Fig. 4-a), whose working principle, design and experimental characterization

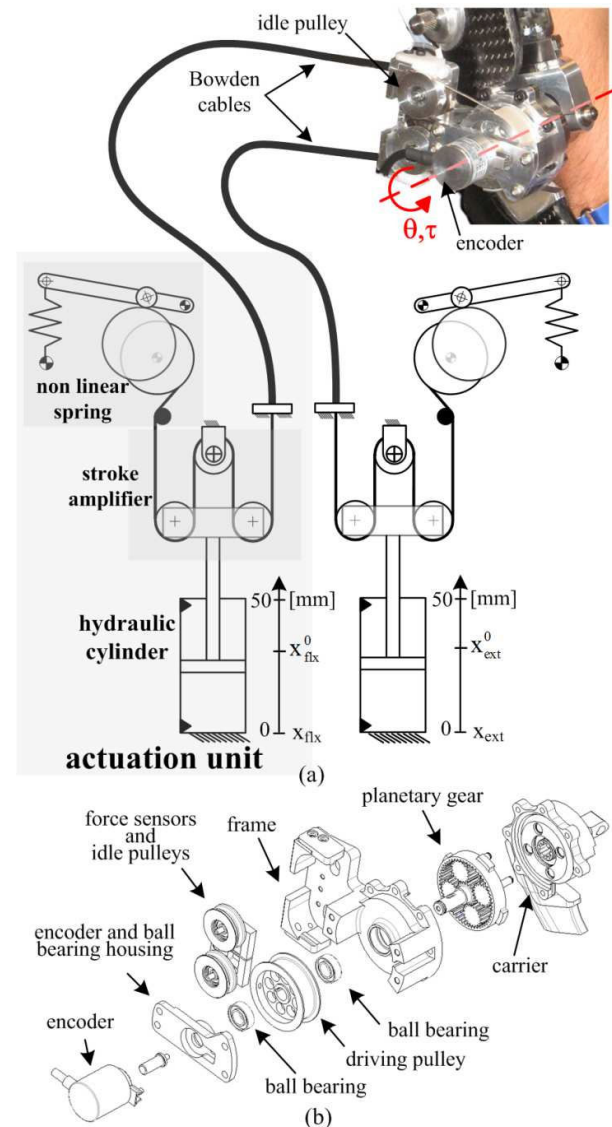


Fig. 2 Antagonistic tendon-driven compliant actuation of the NEUROExos: (a) two remote antagonistic units, named flexor ('flx') and extensor ('ext'), power the NEUROExos active joint, (b) exploded view of the driving block.

have been described in details in [32]. In Fig. 4-b an exploded view of the driving block is illustrated. It is composed by the driving pulley (radius of 19 millimeters), which the antagonistic steel ropes wrap around, a custom-made planetary gear amplifying the input torque of a factor four, the frame housing the force sensors, and two mechanical end stops which limit the range movement of NEUROExos to 130° deg, preventing the human elbow hyper-extension and hyper-flexion.

The planetary gear reduces the force transmitted by each antagonist cable, and consequently, the friction loss due to Bowden cables, as outlined in [33]. The maximum nominal output torque of the driving unit is limited to 15 N·m by the mechanical strength of the planetary gear.

D. Sensory Apparatus and Control Unit

A 1024 ppr incremental optical encoder (2420, Kübler, Germany) was assembled coaxially with the driving pulley (see Fig. 4) and the sun gear to measure the flexion-extension rotation angle (resolution of 0.09°). Two custom load cells allow to measure the force transmitted by the antagonist tendon cables. Finally, linear potentiometers (SLS095, Penny&Giles, Dorset, UK) are used for the measurement of the pistons positions with an accuracy of 0.01 millimetres. The NEUROExos control algorithms runs on a real-time control system (NI PXI-8196 RT, Austin, TX, USA) equipped with a data acquisition card (NI M-series, Austin, TX, USA).

III. THE CONTROL SYSTEM

This section provides a mathematical description of the passive-compliance control strategy showing how it is possible to actively tune the NEUROExos joint equilibrium position and stiffness, thanks to the non-linearity of the antagonist compliant elements.

The torque τ applied by the antagonistic cables on the NEUROExos actuated joint is:

$$\tau = a_{pg} r_{dp} (F_{flx} - F_{ext}) \quad (1)$$

where r_{dp} is the radius of the driving pulley, a_{pg} is the transmission ratio of the planetary gear, and F_{flx} and F_{ext} are the force applied by the extensor and flexor units respectively. Assuming the steel cable infinitively stiff, the total elongation Δl of the transmission line coincides with the strain of the non-linear elastic element and, consequently, the force driven by each cable is a non-linear function of the spring elongation:

$$\begin{aligned} F_{ext}(\Delta l_{ext}) &= b_1 \Delta l_{ext}^2 + b_2 \Delta l_{ext}^2 \\ F_{flx}(\Delta l_{flx}) &= b_1 \Delta l_{flx}^2 + b_2 \Delta l_{flx}^2 \end{aligned} \quad (2)$$

The elongation Δl , of each actuation unit, depends linearly on both the piston position x and the joint angle θ :

$$\begin{aligned} \Delta l_{ext} &= a_s (x_{ext}^0 - x_{ext}) + r_{dp} a_{pg} (\theta - \theta_0) \\ \Delta l_{flx} &= a_s (x_{flx}^0 - x_{flx}) - r_{dp} a_{pg} (\theta - \theta_0) \end{aligned} \quad (3)$$

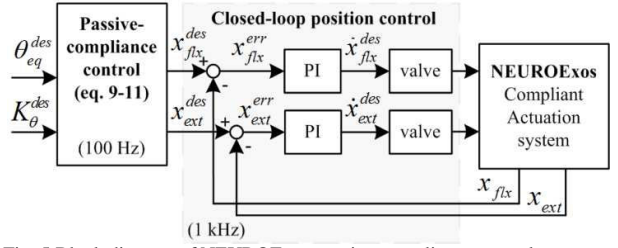


Fig. 5 Block diagram of NEUROExos passive compliance control.

where a_s is the gain of the stroke-amplifier, x_{ext} and x_{flx} are the pistons positions of the extensor and flexor units respectively, θ_0 is a fixed reference angle, and x_{ext}^0 and x_{flx}^0 are the positions for which the elongations Δl_{ext} and Δl_{flx} are nil when $\theta = \theta_0$ ($\theta_0 = 0$ corresponds to the configuration of maximum extension).

The joint equilibrium position θ_{eq} is easily calculated by making $\tau = 0$, and substituting (3) in (2):

$$\theta_{eq} = \frac{a_s (\Delta x_{flx} - \Delta x_{ext})}{2a_{pg} r_{dp}} \quad (4)$$

where $\Delta x_{flx} \triangleq \Delta x_{flx}^0 - x_{flx}$ and $\Delta x_{ext} \triangleq \Delta x_{ext}^0 - x_{ext}$. By appropriately changing the reference frames for the piston positions, it is possible to have $x_{flx}^0 = x_{ext}^0 = 0$, so that (4) becomes:

$$\theta_{eq} = \frac{a_s (x_{ext} - x_{flx})}{2a_{pg} r_{dp}} \quad (5)$$

The joint stiffness, (i.e. $K_\theta \triangleq -\partial \tau / \partial \theta$) is equal to:

$$K_\theta \triangleq 2a_{pg}^2 r_{dp}^2 (b_2 - b_1 a_s (x_{ext} + x_{flx})) \quad (6)$$

As equations (5) and (6) show, the joint position is proportional to $(x_{ext} - x_{flx})$ while the joint stiffness is proportional to $(x_{ext} + x_{flx})$. Thereby, the joint position and stiffness can be regulated independently. Given the desired joint position and stiffness, the high-level layer of the passive-compliance control calculates the desired pistons positions of both the flexor and extensor units, by using two new control variables, which are a linear combination of x_{ext} and x_{flx} . The first variable, namely *differential-mode command*, is defined as a reciprocal shift of the antagonist pistons:

$$x_{dif} = \frac{x_{ext} - x_{flx}}{2} \quad (7)$$

The second, namely *common-mode command*, is an equal shift of the antagonist pistons:

$$x_{com} = -\frac{x_{ext} + x_{flx}}{2} \quad (8)$$

Substituting (7) and (8) into (5) and (6), we get the final equations describing how differential- and common-mode commands can be used to respectively control the joint position (9) and stiffness (10):

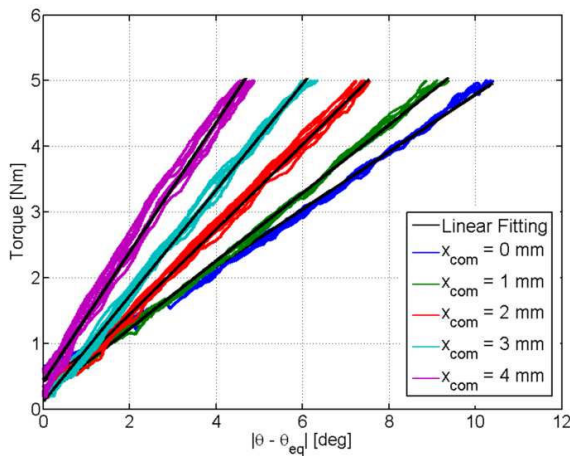


Fig. 6 Static characterization results.

TABLE I
STATIC CHARACTERIZATION - FITTING RESULTS

x_{com} [mm]	0	1	2	3	4
K_θ [Nm/deg]	0.43	0.51	0.64	0.81	0.99
RMSE [Nm]	0.06	0.04	0.07	0.06	0.13

$$x_{dif} = \frac{a_{pg} r_{dp}}{a_s} \theta_{eq} \quad (9)$$

$$x_{com} = \frac{K_\theta - 2a_{pg}^2 r_{dp}^2 b_2}{4a_{pg}^2 r_{dp}^2 a_s b_1} \quad (10)$$

Then, the desired pistons positions are calculated as:

$$\begin{aligned} x_{flx} &= -x_{dif} - x_{com} \\ x_{ext} &= x_{dif} - x_{com} \end{aligned} \quad (11)$$

Finally, the low-level layer controls the hydraulic pistons positions x_{ext} and x_{flx} by means of two independent PID closed-loop compensators (see Fig. 5).

IV. EXPERIMENTAL CHARACTERIZATION

In order to evaluate the performance of the open-loop position and stiffness control, we performed both a static and a dynamic characterization.

A. Static Characterization

The static characterization aims to verify how the NEUROExos control can change the joint stiffness, and how this impacts the static passive behavior of the joint. To this end, we first set the equilibrium position to $\theta_{eq} = 45\text{deg}$, then, for five different values of common mode command (i.e. $x_{com} \in [0, 1, 2, 3, 4\text{mm}]$), we slowly and manually displaced the NEUROExos joint of about 15 deg in both directions (i.e. $\Delta\theta \in [-15; 15]$), while recording at the same time the output of the two cable force sensors. For each value of x_{com} the procedure was iterated ten times in both flexion and extension directions.

The results of this characterization are shown in Fig. 6.

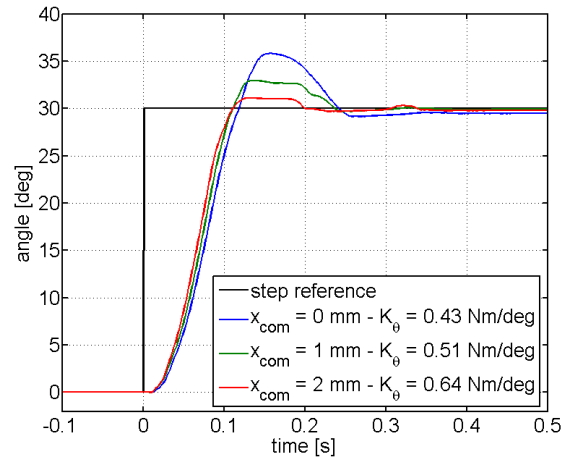


Fig. 7 Step response results.

TABLE II
ANGULAR STEP RESPONSE RESULTS

x_{com} [mm] - K_θ [Nm/deg]	0 - 0.43	1 - 0.51	2 - 0.64
Raising time [s]	0.071	0.067	0.064
Steady-state error [deg]	0.51	0.23	0.12

The measured torque increases linearly with the angular error, defined as the difference between the equilibrium position and the actual position (i.e. $|\Delta\theta| = |\theta_{eq} - \theta|$).

Moreover, an increase of the common mode command results in a higher slope of the torque vs. angular error curve, and therefore, in an increased passive joint stiffness. The estimates of the joint stiffness for the five common-mode commands have been obtained by fitting each curve of Fig. 6 with a linear interpolator. The fitting results, along with the RMSE are reported in Table 1.

B. Dynamic Characterization

In order to have a complete dynamical characterization of the open-loop position and stiffness controller, we analyzed the response to an angular step and chirp commands, under three different common mode command values.

1) Step Response

A 30 deg step (ranging from 0 to 30 deg) was chosen as the desired joint angle input. Three stiffness levels were tested by setting x_{com} equal to 0, 1 and 2 mm. Twenty consecutive steps were performed for each stiffness level. Fig. 7 shows the angular trajectory averaged over all the iterations for each stiffness level. As can be seen from the values reported in Table 2, the raising time decreases proportionally with the increase of the joint stiffness. Moreover, there is a steady-state error which decreases with the level of stiffness (see Table 2). This error is due to the fact that the compliant position controller acts in an open loop fashion, and cannot reject the torque disturbance due to gravity.

2) Chirp Response

The frequency response of the position controller was characterized by means of a linear angular position chirp with a frequency range of 0-8 Hz, a duration of 480 s and an

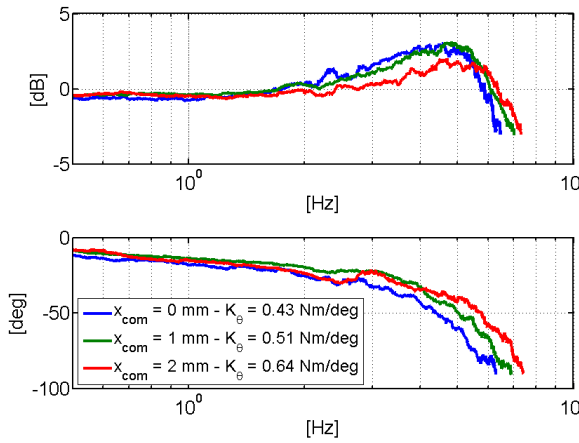


Fig. 8 Estimated Bode diagram of the NEUROExos actuation system.

TABLE III
ANGULAR CHIRP RESPONSE RESULTS

$x_{com}[mm] - K_{\theta}[Nm/deg]$	0 – 0.43	1 – 0.51	2 – 0.64
-3dB bandwidth [Hz]	6.45	6.91	7.24
-3 dB phase [deg]	93.1	89.5	85.8

amplitude of 30 deg (reference angle spans from 45 to 75 deg). The same chirp input was repeated for three different stiffness levels ($x_{com} \in [0, 1, 2\text{mm}]$) in order to evaluate the effect of the stiffness on the system dynamical response. The estimated Bode diagram (amplitude and phase) of the system was obtained as the ratio between the Fourier transforms of actual angular position and the reference angular trajectory. As can be seen from Fig. 8, by increasing the joint stiffness the -3dB bandwidth of the system increases as well (see Table III).

V. PROTOTYPICAL REHABILITATION TASK

A. Prototypical rehabilitation task

In order to evaluate the functionality of the NEUROExos system along with its compliant actuation, a prototypical task has been designed and tested on a healthy volunteer (male, 27 years old, 70Kg). This task aims to simulate a simple rehabilitation procedure, where the subject is totally passive and the exoskeleton drives his arm. NEUROExos was programmed to move the user's arm along a sine wave angular trajectory (amplitude 105 deg, from 10 to 105 deg, frequency 0.5 Hz). A two-minute movement was repeated for four levels of joint stiffness, obtained by setting the common-mode command to 0, 1, 2, 3 mm. Fig. 9 shows the resulting desired and actual angular trajectories for the four levels of stiffness. For the sake of clarity, only one sine wave period is shown. It can be seen that there is an angular error between the reference and the actual trajectory, which mainly results from the effect of the limb weight on the compliant actuation. Most importantly, by increasing the joint stiffness, the error between the reference and the actual trajectory is reduced. This is more evident in Fig. 10, which reports the mean and standard deviation of the amplitude of the actual angular trajectory and the RMSE between the

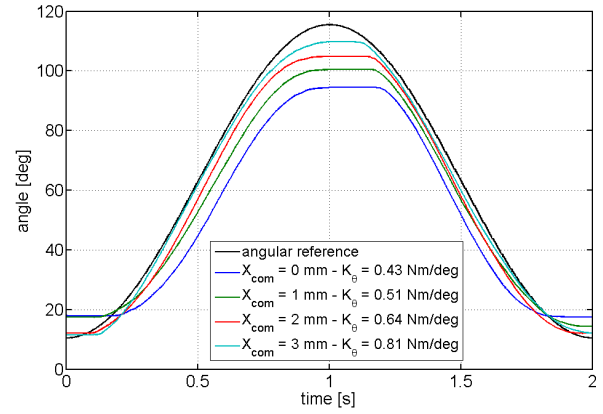


Fig. 9 Prototypical rehabilitation task results.

reference and the actual trajectory for the four levels of joint stiffness. This simple experiment proves that by regulating the joint stiffness, NEUROExos can allow different error levels with respect to the desired trajectory. This variable compliance is a basic feature for a rehabilitative device in order to adapt to the specific level of impairment of the patient [34].

B. Spasmodic movement simulation

As stated in the introduction, one of the main reasons for using a compliant actuation system is the safety of the patient. A spasm, i.e. an involuntary contraction of a muscle or a group of muscles, is a frequent event during the early phase of the rehabilitation. Ideally, the rehabilitative device should detect the spasm and react timely to reduce the interaction force/torque. This is particularly critical when the spasm results in a disturbance that cannot be rejected by the controller (e.g. with frequency components above the disturbance-rejection bandwidth of the closed-loop controller). NEUROExos avoids this problem by relying on the intrinsic compliant feature of its actuation system. In this case, it is possible to regulate the reaction of the exoskeleton to a sudden movement of the user through the actively controllable passive stiffness. In order to prove this concept, we simulate the effect of a spasmodic motion during a prototypical rehabilitation task. In detail, NEUROExos is programmed to perform 40 deg sine wave movements (ranging from 40 to 80, frequency 0.5 Hz, common mode

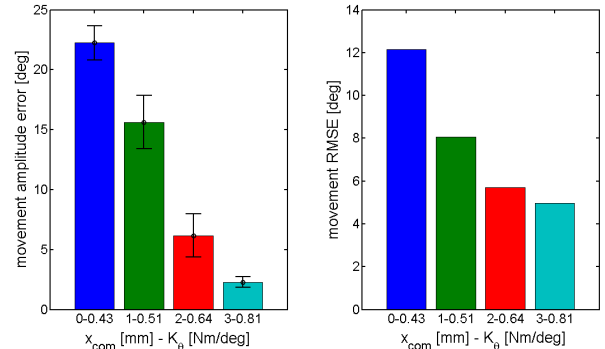


Fig. 10 Movement amplitude and RMSE resulting from the prototypical rehabilitation task

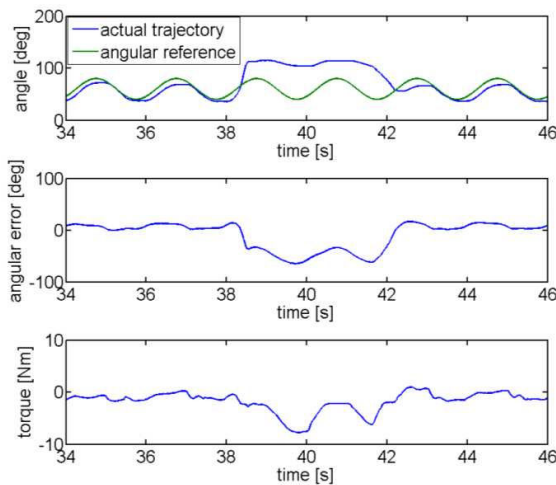


Fig. 11 Reaction of the system to a simulated spasmodic movement.

command 0 mm) independently to the external disturbances. During the movement, the subject wearing NEUROExos is asked to suddenly flex his arm as fast as possible, and maintain the muscle contraction for few seconds, then releases the arm and returns to the passive state. The resulting angular trajectory (both the desired and the actual one) along with the angular error and the measured interaction joint torque are reported in Fig. 11. As expected, even if the robot was not programmed to react to the "simulated" spasmodic event, the measured interaction torque keeps very low (under 8 Nm) and, most importantly, no torque peaks effects are present, thanks to the passive compliance of the actuation.

VI. CONCLUSION

In this paper, we presented NEUROExos, a novel robotic elbow rehabilitation device. This exoskeleton possesses three main innovative features: the double-shell structured links, the four-DoF passive mechanism to align the actuated joint axis to the anatomical elbow axis and a compliant antagonistic actuation system, inspired to the muscle-skeletal apparatus. These features address three important design requirements for a dependable rehabilitation device: (1) a wide and comfortable human-robot interface which can gently transmit the interaction torque, (2) the kinematic compatibility between the human and the exoskeleton, to ensure a proper torque transmission to the human joint without the risk of overloading the patient's articulations, (3) a safe actuation system, which can provide the needed joint torque with a low output impedance over the whole frequency range of possible inputs. In particular, the static and dynamic characterizations of the NEUROExos actuation system demonstrate its ability to independently regulate the passive joint stiffness and the equilibrium position. This feature was then exploited to a prototypical rehabilitation procedure. The arm of a subject wearing the exoskeleton is moved on a reference trajectory by means of an impedance field. Experimental results clearly show that by increasing the joint stiffness level, the arm can be moved along the

reference trajectory with lower angular error. Moreover, the reaction of the system to a spasmodic movement has been tested in order to prove the safety of the system in an application scenario which is common during rehabilitation therapy. Even in this critical situation, NEUROExos shows the benefit of its compliant actuation system. Indeed, the interaction torque remains very low during all the spasm duration.

ACKNOWLEDGMENT

Authors would like to thank Emanuele Cattin and Francesco Giovacchini for their valuable work and support.

REFERENCES

- [1] The world health report 2008, <http://www.who.int/whr/2008/en>
- [2] T. Ingall, "Stroke-Incidence, mortality, morbidity and risk", *Journal of Insurance Medicine*, vol. 36(2), pp. 143-152, 2004.
- [3] T. Truelsen, B. Piechowski-Jozwiak, R. Bonita, C. Mathers, J. Bogousslavsky, and G. Boysen, "Stroke incidence and prevalence in Europe: a review of available data", *European Journal of Neurology*, vol. 13, pp. 581-598, 2006.
- [4] Healthy ageing: keystone for a sustainable Europe, http://ec.europa.eu/health7ph_information/indicators/docs, 2007.
- [5] G. Prange, M. Jannink, C. Groothuis-Oudshoorn, H. Hermens, and M. Ilzerman, "Systematic review of the effect of robot-aided therapy on recovery of the hemiparetic arm after stroke", *Journal of Rehabilitation Research and Development*, vol. 43(2), pp. 171-184, 2006.
- [6] Barreca, S.L. Wolf, S. Fasoli, and R. Bohannon, "Treatment interventions for the paretic upper limb of stroke survivors: a critical review", *Neurorehabilitation and Neural Repair*, vol. 17(4), pp. 220-226, 2003.
- [7] G. Kwakkel, B. Kollen, and H. Krebs, "Effects of robot-assisted therapy on upper limb recovery after stroke: A systematic review", *Neurorehabilitation and Neural Repair*, vol. 22, pp.111-121, 2007.
- [8] H.I. Krebs, N. Hogan, M.L. Aisen, and B.T. Volpe, "Robot-Aided Neurorehabilitation", *IEEE Transactions on Rehabilitation Engineering* vol. 6(1), pp. 75-87, 1998.
- [9] A. Stienen, E. Hekman, F. Van der Helm, G. Prange, M. Jannink, A. Aalsm, and H. Van der Kooij, "Freebal: Dedicated gravity compensation for the upper extremities", in *Proc. of the International Conference on Rehabilitation Robotics*, Noordwijk, The Netherlands, pp. 804-808, 2007.
- [10] R. Loureiro, F. Amirabdollahian, M. Topping, B. Dressen, W. Harwin; "Upper Limb Robot Mediated Stroke Therapy – GENTLE/s Approach" *Autonomous Robot*, vol.15(1), pp. 35-51, 2003.
- [11] G.R. Johnson, D.A. Carus, G. Parrini, S.S. Marchese, and R. Valeggi, "The design of a five-degree-of-freedom powered orthosis for the upper limb", in *Proc. Inst. Mech. Engrs, Part H*, vol. 215, 2001, pp. 275-284.
- [12] Dollar A.M.; Herr H. Lower Extremity Exoskeletons and Active Orthoses: Challenges and State-of-the-Art. *IEEE Transactions on Robotics*. 2008, 24, 144-158.
- [13] A.H.A. Stienen, E.E.G. Hekman, F.C.T. van der Helm, and H. van der Kooij, "Self-Aligning Exoskeleton Axes Through Decoupling of Joint Rotations and Translations, *IEEE Transactions on Robotics*, vol. 25(3), pp. 628-633, 2009.
- [14] J.L.Pons, Rehabilitation Exoskeletal Robotics, *Engineering in Medicine and Biology Magazine, IEEE*, vol.29, no.3, pp.57-63, May-June 2010 doi: 10.1109/MEMB.2010.936548.
- [15] N.G. Tsagarakis and D.G. Caldwell, "Development and Control of a 'Soft-Actuated' Exoskeleton for Use in Physiotherapy and Training", *Autonomous Robots*, vol. 15, pp. 21-23, 2003.
- [16] J. Gonzalez, A. Garcia, M. Vivas, E. Ferrus, E. Alcantara, A. Forner, A new portable method for the measurement of pressure discomfort threshold (ptd) on the foot plant, *Proceedings 4th Symposium on Footwear Biomechanics*, Canmore, Canada, 1999.

- [17] S. Roccella, E. Cattin, N. Vitiello, F. Giovacchini, F. Vecchi, M.C. Carrozza, "Wearable mechatronic device", Pub. No. WO/2009/016478, 2009.
- [18] T. Lenzi, S. De Rossi, N. Vitiello, A. Chiri, S. Roccella, F. Giovacchini, F. Vecchi, M.C. Carrozza, "The neuro-robotics paradigm: NEURARM, NEUROExos, HANDEXOS", in *Proc. of the International Conference of the IEEE Engineering in Medicine and Biology Society*, Minneapolis, US, pp. 2430-2433, 2009.
- [19] M. Bottlang, S.M. Madey, C.M. Steyers, J.L. Marsh, and T.D. Brown, "Assessment of elbow joint kinematics in passive motion by electromagnetic motion tracking", *Journal of Orthopaedic Research*, vol. 18, pp. 195-201, 2000.
- [20] N. Vitiello, T. Lenzi, E. Cattin, S.M.M. De Rossi, S. Roccella, F. Giovacchini, F. Vecchi, M.C. Carrozza, NEUROExos: a mechatronics elbow exoskeleton, in preparation for IEEE Transaction on Mechatronics.
- [21] P. Morasso, M. Casadio, P. Giannoni, L. Masia, V. Sanguineti, V. Squeri, E. Vergaro, Desirable features of a "humanoid" robot-therapist, Annual International Conference of the IEEE Engineering in Medicine and Biology Society, EMBC 2009, pp. 2418-2421, 3-6 Sept. 2009.
- [22] Filippini, R.; Sen, S.; Bicchi, A.; , "Toward soft robots you can depend on," *Robotics & Automation Magazine*, IEEE , vol.15, no.3, pp.31-41, September 2008. doi: 10.1109/MRA.2008.927696.
- [23] Pratt and M.M. Williamson, "Series elastic actuators", in *Proc. of the IEEE International Conference on Intelligent Robots and Systems*, Pittsburgh, US, pp. 339-406.
- [24] J.F. Veneman, R. Ekkelenkamp, R. Kruidhof, F.C.T. van der Helm, and H. van der Kooij, "A Series Elastic- and Bowden-Cable-Based Actuation of Use Torque Actuator in Exoskeleton-Type Robots", *The International Journal of Robotics Research*, vol. 25(3), pp. 261-281, 2006.
- [25] M. Zinn, O. Khatib, B. Roth, and J.K. Salisbury, "A New Actuation Approach for Human-Friendly Robot Design", *The International Journal of Robotics Research*, vol. 23(4-5), pp.379-398, 2004.
- [26] A. Bicchi and G. Tonietti, "Fast and Soft Arm Tactics: Dealing with the Safety-Performance Trade-Off in Robot Arms Design and Control", *IEEE Robotics and Automation Magazine*, 11(2):22-33, 2004.
- [27] B. Vanderborght, R. Van Ham, D. Lefeber, T. Sugar, K. W. Hollander, Comparison of Mechanical Design and Energy Consumption of Adaptable, Passive-compliant Actuators. *The International Journal of Robotics Research*, 28(1): pp. 90-103, 2009.
- [28] A. Polit, E. Bizzi, Characteristics of motor programs underlying arm movements in monkeys, *Journal of Neurophysiology*, 42: pp. 183-194, 1979.
- [29] A. G. Feldman, Functional tuning of the nervous system with control of movement or maintenance of steady posture, II: controllable parameters of the muscles, *Biophysics*, 11:565-578, 1966.
- [30] N. Vitiello, E. Cattin, S. Roccella, F. Giovacchini, F. Vecchi, M.C. Carrozza, and P. Dario, "The NEURARM towards a Platform for Joint Neuroscience Experiments on Human Motion Control Theories", in *Proc. IEEE International Conference on Intelligent Robots and Systems*, San Diego, pp. 1852-1857, 2007.
- [31] N. Vitiello, T. Lenzi, J. McIntyre, S. Roccella, E. Cattin, F. Vecchi, M.C. Carrozza, "Characterization of the NEURARM bio-inspired joint position and stiffness open loop controller", in *Proc. of the 2nd IEEE RAS & EMBS International Conference on Biomedical Robotics and Biomechanics*, pp. 138-143, 2008.
- [32] N. Vitiello, T. Lenzi, S.M.M. De Rossi, S. Roccella, M.C. Carrozza, "A sensorless torque control for Antagonistic Driven Compliant Joints", *Mechatronics*, vol. 20(3), pp. 355-367, 2010.
- [33] A. Schiele, P. Letier, R. van der Linde, F. van der Helm, "Bowden cable actuator for force-feedback exoskeletons", in *Proc. of IEEE International Conference on Intelligent Robots and Systems*, pp. 3599-3604, 2006.
- [34] H.I. Krebs, J.J. Palazzolo, L. Dipietro, M. Ferraro, J. Krol, K. Rankelev, B.T. Volpe and N. Hogan, Rehabilitation Robotics: Performance-Based Progressive Robot-Assisted Therapy Autonomous Robots, Vol. 15, Num. 1, 7-20, DOI: 10.1023/A:1024494031121.